RSC Advances

ROYAL SOCIETY OF CHEMISTRY

www.rsc.org/advances

Cite this: DOI: 10.1039/c0xx00000x

www.rsc.org/xxxxxx

ARTICLE TYPE

Fabrication of NiTe films by transformed electrodeposited Te thin films on Ni foils and their electrical property

Yannan Mu[a.b], Qian Li[a], Pin Lv[a], Yanli Chen[a], Dong Ding[a], Shi Su[a], Liying Zhou[a], Wuyou Fu[a] and Haibin Yang*[a]

Received (in XXX, XXX) Xth XXXXXXXXX 20XX, Accepted Xth XXXXXXXXX 20XX
DOI: 10.1039/b000000x

The compact NiTe thin film was prepared by simple two steps. The high-density vertically tellurium (Te) pillars film (Te source) was synthesized by a rapid and convenient electrodeposition method without any external agent for the first time. Ni_xTe as ohmic contact layer material was obtained by a low temperature heat treatment of Te thin film deposited on Ni substrate. The structural, morphology, optical and electrical properties of as-prepared thin films were examined. I-V characteristic shows that all of the Ni_xTe/Ni samples have already formed ohmic contacts. And NiTe/Ni shows smaller contact resistance than other samples, which suggests its potential application in solar cells on flexible Ni substrate.

1. Introduction

Tellurium (Te), an important p-type narrow band gap semiconductor, has been widely studied owing to their unique useful properties, such as photoconductivity, piezoelectricity, thermoelectricity, nonlinear optical responses and photoelectricity.[1-5] At present, the morphology of Te nanocrystals including nanorod, nanowire, nanobelt, nanotube, nanoplate, flower-like and feather-like has been successfully synthesized by several methods, such as electrochemical deposition, hydrothermal method, solvothermal method, physical vapor deposition and microwave-assisted synthesis. [6-17] It is well known that, for device in practical applications, ordering of nanostructures assembled into arrays on a conducting substrate are required. In this regard, the fabrication of aligned Te pillars on conducting substrates remains challenging. Compared with other methods, electrochemical deposition has the advantages such as high material incorporation, simple technique and low energy consumption.18 Therefore, the electrochemical deposition method has been widely used to fabricate the Te nanocrystals by many researchers. [13, 19] In addition, as a promising template to fabricate tellurides with various novel nanostructures, Te nanocrystals have become a subject of intensive research. Zhu et al synthesized Ag_2Te nanoribbons in the same shape and similar size through the reaction of Ag with tri-wing Te nanoribbons as the precursor and template.[20] Furthermore, Te can react readily with other elements to generate a wealth of functional materials such as NiTe[21], Bi_2Te_3[3, 5], CdTe[22], PbTe[23], ZnTe[24], and HgCdTe[25]. These Te nanostructure materials have wide applications in diverse fields such as thermoelectric material, light emitting diodes, solar cells, and microwave devices infrared detector.

Nickel telluride (NiTe), an important intermetallic compound with a nickel-arsenide-type (NiAs type) crystal structure, has attracted great interest for its electric, magnetic, crystallographic (helical-chain conformation) and thermodynamic properties.[26-30] In 1938, Tengnér asserted the existence of a continuous solid-solution range between the compounds NiTe and $NiTe_2$. He suggested that in proceeding from NiTe (NiAs type) to $NiTe_2$ (Cd(OH) type).[31] It is important to point out that NiTe can be used as ohmic contacting layer of II–VI semiconductors for their distinctive electrical transport property.[32] Traditionally, the method used to prepare NiTe is the direct combination of the nickel and tellurium elements in evacuated silica tubes at high temperature （600 °C） for several hours. [7] In addition, Zhang et al. have prepared NiTe nanocrystallites by hydrothermal method with hydrazine hydrate as a reducer[33]. Nevertheless, the mentioned methods for preparing NiTe have some disadvantages, such as toxic, high energy consumption and relatively long reaction times. Hence, environmental friendly, energy saving and convenient methods should be sought for commercial production.

In this work, we explored a simple method to prepared NiTe. Firstly, we presented a simple one-step, environmental friendly and template-free electrochemical deposition method to deposit Te thin film at room temperature without any external agent. Subsquently, we obtained the NiTe thin film by calcinating as-prepared Te thin film (Te source) on Ni substrate (Ni source) at 350 °C. It is worth mentioning that the study displays three advantages using this method to prepare chalcogenide compounds: (1) selection of single Te source electrolyte avoids complications involved with codeposition of the elements and impurities; (2) a graphite plate insteat of conventional Platinum (Pt) is used as counter electrode for Pt may dissolve into electrolyte and thus influence the reaction on working electrode; [34] (3) compared with other reports, [35-38] crystalline products can be obtained by a thermal transformation step. Furthermore, the electrical properties of NiTe/Ni indicate that it would have potential application as back contacting layer in solar cells.

2. Experimental section

2.1 Preparation of Te pillars film

Before performing the experiment, the Ni foil (1.5×4 cm^2) had been pretreated by an ultrasonic cleaner for 30 min in isopropanol, acetone, anhydrous ethanol and double-distilled water respectively. Degreased Ni substrates were dried by under N_2 .The electrochemical experiments were carried out in a single compartment three-electrode cell in air atmosphere. A cleaned Ni foil, a saturated silver/silver chloride (Ag/AgCl) electrode and a graphite plate were used as the working electrode, reference electrode and counter electrode, respectively. Te thin film was deposited in an acidic electrolytic bath containing 0.01 M sodium tellurite (Na_2TeO_3) and 1M nitric acid (HNO_3). Na_2TeO_3 and HNO_3 were analytical grade and were used as purchased without further purification. Double-distilled water was used as solvent in the experiment. In the electrochemical experiment, the applied potential was optimized at −0.30 V (vs. Ag/AgCl) and the deposited time was 300 s. The reaction temperature was kept constant at room temperature. Subsequently, the as-prepared Te thin film was washed with double-distilled water and dried under dried N_2.

2.2 Preparation of NiTe film

Firstly, the obtained Te thin film was put in a porcelain boat, and then the porcelain boat was placed at the center of the muffle furnace, which was full of N_2.The muffle furnace heated up to different temperatures (250 ^oC, 300 ^oC, 350 ^oC, 400 ^oC) at a rate of 25 ^oC min^{-1}. After a reaction time of 30 min, the furnace was switched off and cooled down to room temperature naturally. NiTe film was obtained when the annealing temperature was 350 ^oC.

2.3 Characterization

Electrochemical studies were made by a potentiostat (CHI electrochemical workstation) with three electrodes. The crystal structures were identified by a Rigaku D/max-2500 X-ray diffractometer (XRD) with Cu Kα radiation (λ = 1.5418 Å). XRD measurement was conducted in the scanning range between 20 ^{o} and 80 ^{o}. A model JEOL JSM-6700 field emission scanning electron microscopy (FESEM) was utilized to investigate the morphology and dimensions of as-prepared samples. Energy dispersive X-ray analysis (EDX) of the NiTe film was performed with an EDAX Genesis 2000 system (FEI Inc) installed on the XL 30 ESEM imaging instrument. The transmission electron microscopy (TEM) and selected area electron diffraction (SAED) pattern were taken on a JEOL JEM-2200FS with an accelerating voltage of 200 kV. A UV-3150 double-beam spectrophotometer was used to characterize the optical absorption spectra at room temperature. A Keithley 2400 Source-Meter was used to characterize the electronic properties of all samples

3. Results and Discussion

Cyclic voltammetry was used to study the electrochemical reactions in the electrolyte solution. Fig.1 shows the cyclic voltammogram of Te^{4+} at room temperature. The potential was changed between +0.30 V and −0.60 V (vs.Ag/AgCl) and the scan rate was 100 mVs^{-1}. One cathodic peak was observed. The cathodic current began to increase gradually at about an applied

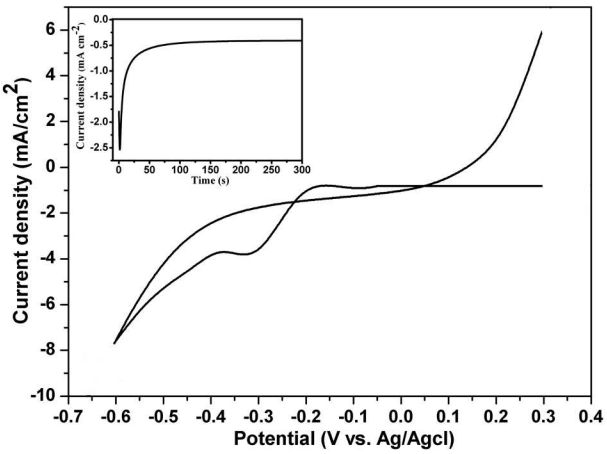

Fig.1 Cyclic voltammogram on Ni substrate in the electrolyte solution containing Na_2TeO_3 (0.01 M) + HNO_3 (1 M) and scan rate is 100 mVs^{-1}; Change in the current density during potentiostatic electrodeposition at −0.30 V vs. Ag/AgCl within 300 s (inset).

potential of −0.18 V versus Ag/AgCl. When the potential was more negative than −0.45 V and more positive than −0.15 V, no products were obtained on Ni substrates. A visible dark gray film appeared on the surface of the Ni foil at a potential about −0.30 V versus Ag/AgCl. It should be attributed to the reduction of TeO_3^{2-}.The mechanism of Te electrodeposition in an acidic solution is described as follows:

$$TeO_3^{2-}+6H^++4e^-\rightarrow Te+3H_2O$$

The change of current density with time is shown in Fig.1 (inset) during the direct current potentiostatic electrodeposition at −0.30 V (vs. Ag/AgCl) for 300 s. It shows that the cathodic current density increases quickly at initial time and decreases gradually. The change of current density within the initial 100 s corresponds to Te nucleation on the Ni foil surface. During electrodeposition, the first process is fast ionization. Subsquently, charge redistributes under the action of the voltage. The current reduced with the extension of deposition time, which is attributed to the resistivity of the deposited film increases. After the attainment of uniform nucleation on the entire surface, the current density became constant and the film growth started.

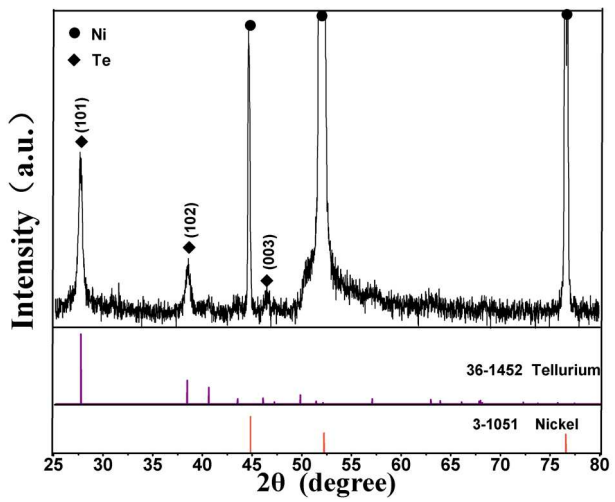

Fig.2 XRD pattern of the as-synthesized Te thin film on Ni substrate.

Fig.2 shows the X-ray diffraction pattern of the Te thin film on the Ni substrate. Besides the diffraction peaks from the Ni substrate denoted by black solid circles, the peaks of the sample can be clearly observed at 27.57 °, 38.24 ° and 45.96 ° as shown in Fig.2, which can be well indexed to the (101), (102), (003) planes of hexagonal phase Te (JCPDS card no. 36-1452). No any other phase can be detected by XRD, which reveals that pure Te is obtained. In addition, the preferred orientation (101) and peaks with small full-width at half-maximum FWHM are indicative of good crystallization of the samples.

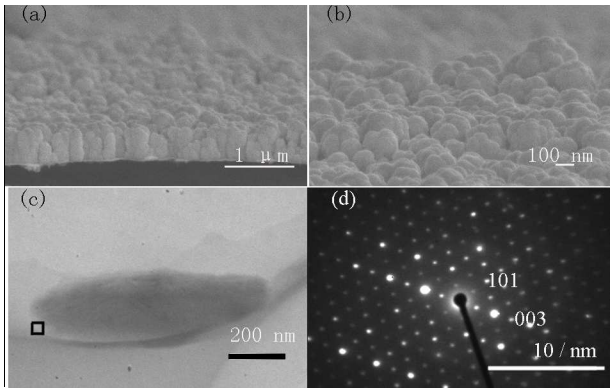

Fig.3 (a) Cross-sectional FESEM image, (b) tilted top-view FESEM image, (c) TEM image of a single Te pillar and (d) SAED pattern of the sample.

Fig.3(a,b) gives FESEM image of the sample, which reveals that the Ni substrate is covered with large-scale pillars, which lengths range from 400 nm to 500 nm. They are oriented vertically with respect to the Ni substrate surface. The surface morphology of as-deposited sample clearly shows that the pillars have a compact and uniform structure. And the surface is rough. The TEM image of a single pillar in Fig.3(c) shows that the Te pillar has a diameter of 250 nm and a length of 500 nm. The selected-area electron diffraction (SAED) taken from a single pillar further confirms the well-crystallized hexagonal phase structure of the pillar (Fig.3(d)). Regular diffraction dots show the single crystal nature of the Te pillar. Surveys of the sample using SAED indicate that these Te pillars are consistently the preferred orientation (101).

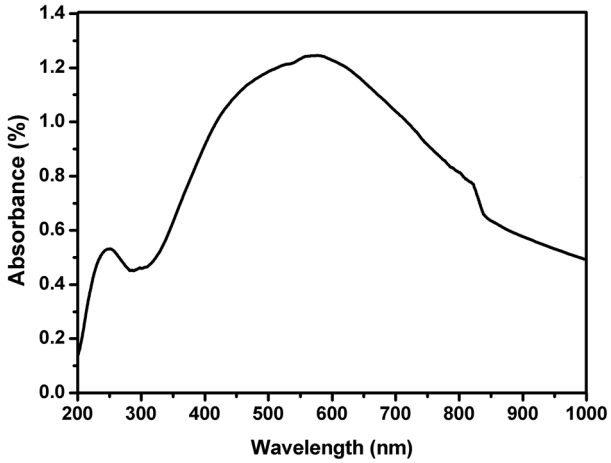

Fig.4 UV–visible absorption spectrum of Te thin film via electrochemical deposition method.

The UV–visible absorption spectrum for the as-deposited Te thin film are shown in Fig.4. The UV-vis absorption bands are quite similar to those reported for by Swan et al and Qian et al [40,41]. As shown in Fig.4, there are two absorption peaks which located at 248 nm and 563 nm. The absorption peak centered at 248 nm is due to the allowed direct transition from the valence band (p-bonding triplet) to the conduction band (p-antibonding triplet), and the other absorption peak at 563 nm can be assigned to a forbidden direction transition.[39-41] However, further research is needed because the origin of this absorption peak is still not clear.[42]

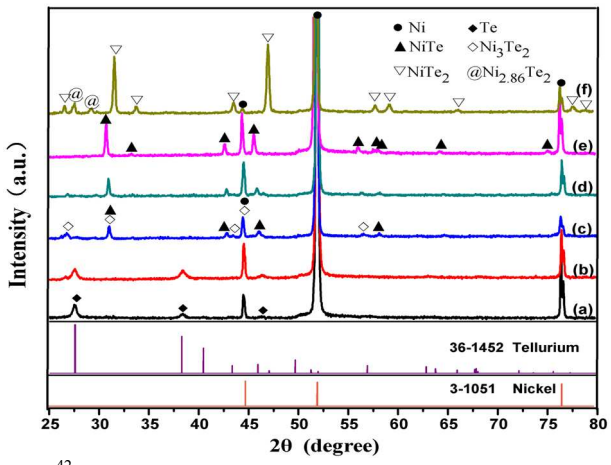

Fig.5 XRD patterns of the samples prepared at different annealing temperature for 30 min: (a) as-prepared Te, (b) 200 °C, (c) 250 °C, (d) 300 °C, (e) 350 °C , (f) 400 °C.

To study the process of Te transform into Ni_xTe in details, a series of experiments have been carried out from 200 °C to 400 °C. Fig.5 displays the XRD patterns of as-prepared samples which were annealed from 200 °C to 400 °C for 30 min in N_2. The results display the process that Te transform into NiTe. As shown

in Fig.5, the phase transformation does not start when annealing temperature is 200 °C. In addition, Fig.5(c) shows that NiTe and Ni_3Te_2 appears accompany with Te phase disappeares when the Te film is sintered at 250 °C for 30 min.With increasing of annealing temperature, the diffraction peak intensity of NiTe, which indicates the crystallinity has improved. At the same time, the diffraction peaks of Ni_3Te_2 weaken gradually until dissappear.

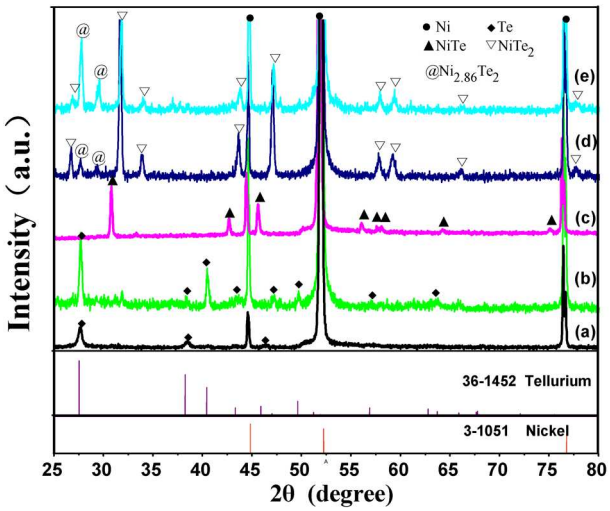

Fig.6 XRD patterns of the samples prepared at 350 °C for different times: (a) as-prepared Te, (b) 15 min, (c) 30 min, (d) 45 min, (e) 60 min.

The result of Fig.5(e) indicates that the diffraction peak position and relative intensities of the prepared samples are well matched with the standard powder diffraction file NiTe (JCPDS 89-2018). No diffraction peaks from other products are surveyed. Furthermore, NiTe transform into ($NiTe_2$ +$Ni_{2.86}Te_2$) completely when the annealing temperature is extended to 400 °C. In addition, the study of a series of annealing time at 350 °C is also carried out. Fig.6 shows the XRD patterns of the samples prepared at 350 °C for different times (0 – 60 min). As shown in Fig.6(b), the products is mainly Te and mixture of some indistinct substances when the annealing time is 15 min. Fig.6(c) shows that Te transform into NiTe completely extending the annealing time to 30 min. With increasing of annealing time to 45 min and 60 min, the reaction products are mainly $NiTe_2$ and mixture of $Ni_{2.86}Te_2$. Above all, annealing temperature and time prompt the reaction and phase transition. Therefore, the reaction condition should be (350 °C, 30 min) to make sure the products we prepared are pure phase and well-crystallized NiTe.

As we known, NiTe can be obtained by hydrothermal and high temperature solid-state reaction,[43,44] which require high energy consumption and relatively long reaction times. In contrast, the reaction temperature and time are only 350 °C and 30 min in our study. There may be interdiffusion of Ni and Te and solid-phase chemical reactions occur. The reaction to form NiTe can be formulated as the following equation:

Ni +Te → NiTe

Based on the XRD result, a general trend of decreasing Ni content (Ni_3Te_2→NiTe→$NiTe_2$) with respect to increasing annealing temperature can be observed. Thus it suggests that as-generated Ni_xTe may prevent further interdiffusion of Ni and Te, which is benefit for photovoltaics because of too much metal outdiffuses to the surface forming defects and recombination centers.[45] As shown in Fig.5(f) and Fig.6(d,e), the increased annealing temperature or prolonged annealing time results that samples include two substances $NiTe_2$ and $Ni_{2.86}Te_2$. The reason for the appearance of $Ni_{2.86}Te_2$ may occur some phase segregation but it needs to be further investigated.

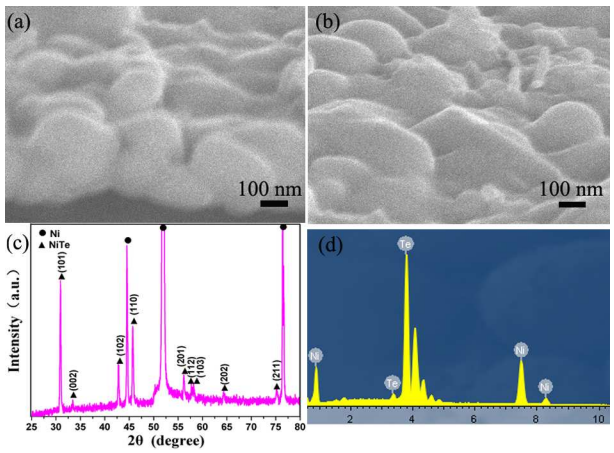

Fig.7 (a)Cross-section FESEM image, (b) tilted top-view FESEM image, (c) XRD and (d) EDX spectra of NiTe thin film.

The XRD, EDX and FESEM spectra of the NiTe thin film through as-deposited Te thin film is observed in Fig.7. Fig.7(a) and (b) shows the cross-section and tilted top-surface FESEM images of the NiTe film, respectively. It is obvious that the morphology of NiTe is dense thin film and the thickness is about 300 nm. Fig. 7(c) shows the XRD pattern of NiTe. All the diffraction peaks can be perfectly indexed to a pure hexagonal phase of NiTe (space group: P63/mmc), which is in good agreement with the standard XRD data (JCPDS 89-2018). The strong and sharp diffraction peaks indicate that the product is well crystallized. No peaks of impurities are detected, revealing that the high purity of NiTe films are fabricated in our experiment. In addition, NiTe has been peeled off from Ni substrate before taking the EDX spectrum. As shown in Fig.7(d), EDX analysis indicates the sample is composed of Ni and Te and the atomic concentration of Ni and Te is 1.02 in agreement with the desired stoichiometric composition of NiTe. All of the results show that NiTe thin film has been successfully prepared through simple calcination of Te thin film deposited on Ni substrate. According to the above results, NiTe and Te are all hexagonal phase. In other words, the crystal structure has not changed during the transformation process.

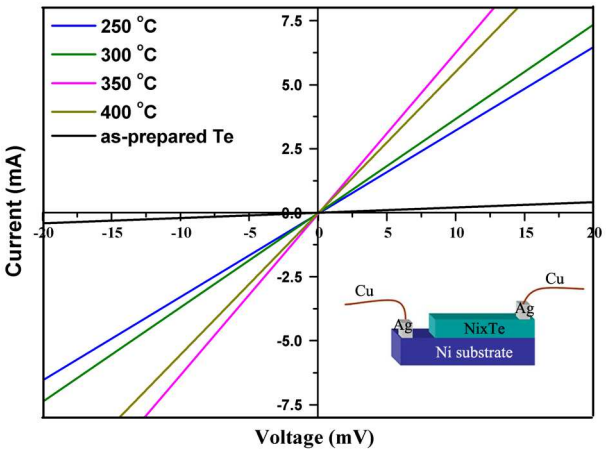

Fig.8 Current voltage (I-V) curves of Ni_xTe/Ni samples annealed at different temperatures. Inset: the structure schematic diagram of electric properties measure.

To characterize the conductive properties of the Ni_xTe /Ni, the electrical contacts were made by attaching copper wires to the surface of the Te or Ni_xTe films with colloidal silver paste as the conductive glue. The schematic diagram is shown in the inset of Fig.8. Fig.8 shows the room temperature I-V characteristic of samples contacts on Ni. The linear I-V curves indicate ohmic contacts. And the slope of I-V curve reveals electroconductibilty. As shown in Fig.8, electroconductibilty is significantly improved by transforming Te into Ni_xTe. When the annealing temperature is higher than 250 °C, all Ni_xTe/Ni samples show linear I-V curves, indicating that ohmic contacts have already been formed on Ni. Furthermore, it is evident that the contact resistivity of sample NixTe/Ni firstly decreases and then increases with the increase of annealing temperature. It is well known that conductive properities depend on the materials. In our study, the heat treatment makes material change (Te→ Ni_3Te_2→NiTe→$NiTe_2$). It is reported that $NiTe_2$ is suited as a back contact layer for solar cell.[46] The slope of I-V curve of sample NiTe/Ni is higher than other samples. The results verify that NiTe/Ni possesses better ohmic contacts characteristics.

Conclusions

In this study, we have prepared the single crystalline hexagonal Te thin film on a Ni substrate by electrochemical deposition method at room temperature. A uniform growth with well-connected pillar morphology can be obtained at −0.30 V. XRD analysis showed that all diffraction peaks in the pattern could be indexed to hexagonal Te, having the preferred orientation (101). Furthermore, it may provide a reference for the preparation of Te thin film on a Ni foil by template-free electrochemical deposition method. As-prepared Te thin film is demonstrated to be an ideal template to prepare other telluride nanocompounds through the successful synthesis of NiTe thin film. The transformation of phases with annealing temperature and time have been studied. The electric properties of Ni_xTe/Ni show that ohmic contacts have already been formed and NiTe/Ni has better electrical properties than other samples. It is expected that these Ni_xTe films could be promisingly applied as back contact layers of solar cells on flexible Ni substrate.

Acknowledgements

This work was financially supported by the Science and Technology Development Program of Jilin Province (no. 20110417), the National Natural Science Foundation of China (no. 51272086) and the Science and Technology Research Project of Heihe University (no. KJY201405). The authors would like to thank Dr. Xiaoming Zhou and Dr. Huizhen Yao for their help and discussion on the manuscripts.

Notes and references

a State Key Laboratory of Superhard Materials, Jilin University, Changchun 130012, PR China
b Department of Physics and Chemistry, Heihe University, Heihe 164300, PR China

Author Information

Corresponding Author

**E-mail: yanghb@jlu.edu.cn*

Fax: +86 431 85168763; Tel: +86 431 85168763;

1 V.B.Anzin,Y.V. Kosichkin, AI Nadezhdinskii, *PHYS STATUS SOLIDI A.*, 1973, **20,** 253.
2 Z.H. Wang, L.L. Wang, J.R. Huang, J. Mater. Chem., 2010, **20,** 2457 .
3 D. Royer, E. Dieulesaint. *J. Appl. Phys.,* 1979, **50**, 4042.
4 D.V. Damodara, N. Jayaprakash, N. Soundararajan. *J MATER SCI.* 1981, **16**, 3331.
5 Y. Wang, Z. Tang, P. Podsiadlo. *Adv. Mater.*, 2006, **18**, 518–522.
6 Z.P. Liu, Z.K. Hu, Q. J. Xie, *Mater. Chem*. 2003, **13**, 159.
7 Q.Y. Lu, F. Gao, S. Komarneni. *Adv. Mater.* 2004, **16**, 1629.
8 B. Zhang, W.Y. Ho, X.C. Ye. *Adv. Funct. Mater.* 2007, **17**, 486.
9 T. Siciliano, E. Filippo, A.Genga, *Sens. Actuators*, B. 2009, **142**, 185.
10 G.H. Li, X.Z. Cui, C.Y. Tan. *RSC Adv.* 2014, **4**, 954.
11 S. Wang, K. Zhang, H. Zhou .*CrystEngComm.* 2010, **12**, 3852.
12 S. Wang, W. Guan, D. Ma. *CrystEngComm*. 2010, **12**, 166.
13 J. Szymczak, S. Legeai, S.Diliberto, *Electrochem. Comm.,* 2012, **24**, 57.
14 C.Z. Yan, C.M. Raghavan, D.J. Kang, *Mater. Lett.,* 2014, **116**, 341.
15 B.J. Xi, S.L. Xiong, H.Fan, *Cryst. Growth Des.,* 2007, **7**,1185.
16 S. Sen, M.B. Umananda, V. Kumar, *Cryst. Growth Des.* 2008, **8** , 238.
17 Y.J. Zhu, W.W. Wang, R.J.Qi, *Angew. Chem.- Int. Edit.* 2004, **43**, 1410.
18 C. Gu, H. Xu, M. Park, and C. Shannon, *Langmuir,* 2009, **25**, 410-414.
19 A. Zhao, L.D. Zhang, Y. Pang, *Appl. Phys. A.* 2005, **80**, 1725.
20 H. Zhu, J. Luo, H. Zhang, J. Liang, G. Rao, J. Li, G. Liu and Z. Du *CrystEngComm*, 2012, **14**, 251.

21 N. Umeyama, M. Tokumoto,A.Yagi, et al., *Jpn.J.Appl.Phys.* 2012, **51**, 053001.

22 S.H. Song, J. Wang, Isshiki, *J.Cryst. Growth.*, 2002, **236**, 165.

23 Y. Yang, D. Taggart, M. Brown, *ACS NANO*, 2009, **3**, 4144-4154.

24 R.Yang,W.Jie,H.Liu, *J. Cryst. Growth*, 2014, **400**, 27-33.

25 K.J. Hong, J.W. Jeong, H.W. Baek, *J. Cryst. Growth*. 2002, **240**, 135.

26 V. P. ZHUZE and A. R. REGEL, *Z. Teckh. Fiz.SSSR*, 1955, **25**, 978.

27 S. FUJIME, M. MURAKAMI and E.HIRAHARA, *J. Phys. Soc. Jpn* 1956, **11**, 327.

28 G.G.DVORYANKINA and Z.G. PINSKER, *Kristallogr.* 1963,**7**, 458.

29 S. A. SHCHUKARER and M.S. APURINA, Russ. *J. Inorg. Chem.* (English translation) 1960, **5**, 1167.

30 E. F. WESTRUM and R. E. MACHOL, *J. Chem. Phys.*,1959, **29**, 824.

31 S. Tengnér, Z. anorg. *u. allgem. Chern*. 1938, **239**, 126 .

32 Q. Peng, Y. Dong and Yadong Li, *Inorg. Chem.*, 2003, **42**, 2174-2175.

33 H.T. Zhang, Y.M. Xiong, X.G. Luo, et al, *J.Cryst. Growth.*, 2002, **242**, 259–262.

34 C. Gu, B. Norris, F. Fan, *ACS Catal*. 2012, **2**, 746−750.

35 G. Pezzatini, S. Caporali, M. Innocenti, M.L. Foresti *J. Electroanal. Chem.,* 1999, **475**, 164–170.

36 B. Gregory, M. Norton and J. Stickney, *J. Electroanal. Chem.*, 1990, **293**, 85-101

37 B. Gregory, John L. Stickney, *J. Electroanal. Chem.*, 1991, **300**, 543-561.

38 F. Karouta, M. Krämer, J. Kwaspen，*ECS trans.*, 2008, **16** , 181-191.

39 H. M. Isomaski, *J. von Boehm. Phys. Scr.* 1982, **25**, 801.

40 R. Swan, A.K. Ray, C. A. Hogarth, *Phys. Status Solidi A.* 1991, **127**, 555.

41 H.S. Qian, S.H. Yu , J.Y. Gong. *Langmuir.* 2006, **22**, 3830.

42 Gautam, U. K.; Rao, C. N. R. *J. Mater. Chem*. 2004, **14**, 2530.

43 H.T. Zhang, Y.M. Xiong, X.G. Luo, C.H. Wang, S.Y. Li, X.H. Chen. , *J.Cryst. Growth.,* 2002, **242**, 259–262.

44 Jan. Barstad, Fredrik. Grφnvold, E. Rφst, et al., *Acta. Chem. Scand*. 1966, **20**, 2865.

45 Lukas Kranz, C.Gretener, J. Perrenoud, et al., *Nat Commun*, 2013, **4**, 2306, DOI: 10.1038/ncomms3306.

46 O.Rotlevi, K.Dobson, D.Rose, *Thin Solid Films*, 2001, **387**, 155-157.